Superconductivity induced by interband nesting in the three-dimensional honeycomb lattice

Seiichiro Onari,[1] Kazuhiko Kuroki,[2] Ryotaro Arita,[1] and Hideo Aoki[1]
[1]*Department of Physics, University of Tokyo, Hongo, Tokyo 113-0033, Japan*
[2]*Department of Applied Physics and Chemistry, University of Electro-Communications, Chofu, Tokyo 182-8585, Japan*
(Received 11 January 2002; published 13 May 2002)

In order to study whether the interband nesting can favor superconductivity arising from electron-electron repulsion in a three-dimensional system, we have looked at the repulsive Hubbard model on a stack of honeycomb (i.e., non-Bravais) lattices with the fluctuation exchange approximation, partly motivated by the superconductivity observed in MgB_2. By systematically changing the shape of Fermi surface with varied band filling n and the third-direction hopping, we have found that the pair scattering across the two bands is indeed found to give rise to gap functions that change sign across the bands and behave as an s or d wave within each band. This implies (a) the electron repulsion can assist *gapful* pairing when a phonon-mechanism pairing exists and (b) the electron repulsion alone, when strong enough, can give rise to a d-wave-like pairing, which should be, for a group-theoretic reason, a time-reversal broken $d+id$ with *point nodes* in the gap.

DOI: 10.1103/PhysRevB.65.184525 PACS number(s): 74.20.Mn

I. INTRODUCTION

The recent discovery of the superconductivity in MgB_2 (Ref. 1) with relatively high transition temperature ($T_c \sim 39$ K) has invoked renewed interests in sp-bonded materials. Electronically, the system is a π electron system on layered honeycomb lattice, which immediately reminds us of graphite intercalation compounds (GIC's) such as LiC_6 (Ref. 2) or KC_8.[3,4]

While the GIC is considered to be a conventional superconductor with $T_c < 5$ K, MgB_2 has an unusually high T_c for sp-bonded materials (with a recent exception of C_{60}-FET structure[5]). Recently, Choi *et al.*[6] have used an *ab initio* pseudopotential density functional theory to solve Eliashberg's equation numerically, and have reproduced $T_c \sim 39$ K, isotope-effect exponent $\alpha_B \sim 0.3$,[7,8] and have obtained a gapful BCS pairing, which is consistent with experimental results such as specific heat,[9,10] tunneling and photoemission spectra,[11–14] penetration depth,[15] and the Raman spectra.[16] Thus GIC and MgB_2 both seem to be mainly phonon-mediated superconductors. However, to realize a high-T_C electron repulsion should not stand in the way of the phonon mechanism, so the question may be paraphrased: can the electron repulsion stand away from or possibly even assist the phonon-mediated pairing.

On a more positive side, superconductivity from electron-electron repulsion itself is fascinating in many ways, but there are many open questions. While there is a growing consensus that high-T_C cuprates may be related to the electron correlation, we are only beginning to understand the link between the underlying band structure and the way in which the electron-mechanism superconductivity appears.[17] Indeed, the way in which the superconductivity occurs is sensitively affected by the shape of the Fermi surface. Recently, two of the present authors proposed[18] that multiband systems should open a new possibility of much higher T_c, where a fully gapped BCS gap function can appear when the Fermi surface consists of disconnected pieces, while the usual wisdom dictates that the repulsion-originated superconductivity should have, as in the cuprates, a strongly anisotropic gap function with nodes. They have conceived and demonstrated that, for some two-dimensional lattice models, the pair scattering (the Coulombic matrix elements that scatter pairs of electrons across the Fermi surface) can occur across the pockets, which gives rise to a gap function that changes sign across the pockets with the same sign within each pocket.

So the purpose of the present paper is a combination of the above two motivations. Namely, we study whether the interband nesting can favor superconductivity arising from electron repulsion in a three-dimensional system, by taking the repulsive Hubbard model on a stack of honeycomb lattices as a prototype. There, the honeycomb, a typical non-Bravais lattice, provides two pieces of the Fermi surface arising from the two bands, while the stacking can provide a natural nesting along that direction. So, if the pair scattering across the two bands along the nesting vector works favorably, we can expect a pairing from the interband nesting with the BCS gap with opposite signs across the two bands.

So we have studied the systematic dependence of the solution of Eliashberg's equation with the multiband fluctuation exchange approximation on the shape of Fermi surface by changing the band filling and the third-direction hopping. The presence of a strong interband nesting is found to indeed give rise to gap functions that change sign across the two bands, but, if we turn to the symmetry within each band, there exist two, nearly degenerate modes that behave, respectively, as s and d waves. This implies (a) the electron repulsion can assist an s-wave-like pairing when the phonon-mechanism pairing exists as a dominant mechanism. We have further found that (b) when the electron repulsion is

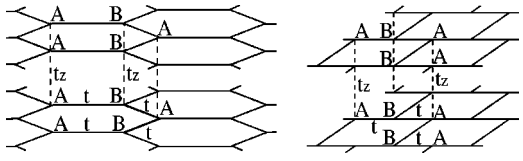

FIG. 1. 3D layered honeycomb lattice (the left panel), which is topologically equivalent to the lattice in the right panel. A and B indicate sublattices.

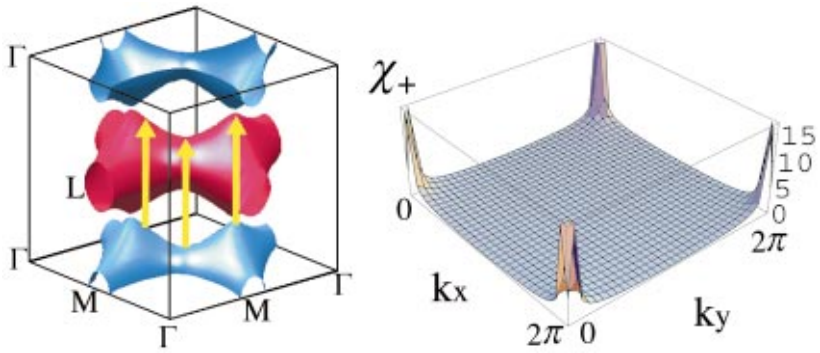

FIG. 2. (Color) Fermi surface (left panel, blue: bonding band, red: antibonding band) and χ_+ (right panel) with $k_z=\pi$ for $U=1.5$, $n=1.03$, $t_z=0.65$, $T=0.01$. Yellow arrows indicate the nesting vector.

strong enough, the *d* wave is realized, which should be, for a group-theoretic reason, a time-reversal broken linear combination of two symmetries with *point* nodes in the gap.

According to the band calculation,[19] the Fermi surface of MgB_2 consists of two tubular networks having a boron-$2p\pi$ character along with two cylinders of the boron-$2p\sigma$ characters. As has been stressed by several authors,[20,21] the nesting between these two π bands are quite good. Although $p\sigma$ bands are considered to be important in that the electron-phonon interaction is much stronger in this band, here we concentrate on the $p\pi$ bands in order to focus on the effects of the Fermi surface nesting. The GIC, on the other hand, has a much smaller interlayer transfer energy (t_z), so that the Fermi surface is a cylinder of carbon π character with no dominant nesting vectors. So in the latter part of the paper we shall cover both MgB_2 and GIC situations in a systematic variation of t_z and band filling. The systematic study also serves to explore how the interband and intraband nesting compete in realizing superconductivity.

II. FORMULATION

Now let us start with the case corresponding to MgB_2. Spin-fluctuation-mediated superconductivity is here studied with the fluctuation exchange approximation (FLEX) developed by Bickers *et al.*[22–25] The model is a 3D two-band Hubbard model with the repulsion U on layered honeycomb lattice

$$\mathcal{H}=\sum_{\langle i,j\rangle,\sigma}\sum_{\alpha,\beta}^{\mathrm{A,B}} t_{ij}(c_{i\sigma}^{\alpha\dagger}c_{j\sigma}^{\beta}+\mathrm{H.c.})+U\sum_i\sum_\alpha n_{i\uparrow}^{\alpha}n_{i\downarrow}^{\alpha}, \quad (1)$$

where U is the Hubbard repulsion. The essential ingredient here is the non-Bravais lattice having *A* and *B* sublattices, which has two bands within a layer. Here we assume a non staggered layer stacking as realized in MgB_2 and GIC (Fig. 1), which also depicts the interlayer hopping t_z. Hereafter we take the intralayer hopping $t=-1$.

The noninteracting band dispersion for 3D honeycomb is

$$\epsilon(\mathbf{k})=2t_z\cos k_z \pm t\sqrt{3+2[\cos k_x+\cos k_y+\cos(k_x+k_y)]}. \quad (2)$$

In the two-band FLEX,[26,27] Green's function G, self-energy Σ, spin susceptibility χ, and the gap function ϕ all become 2×2 matrices, such as $G_{\alpha\beta}(k)$, where $k\equiv(\mathbf{k},i\omega_n)$ with $\omega_n=(2n-1)\pi T$ being the Matsubara frequency for fermions.

The self-energy is given by

$$\Sigma_{\alpha\beta}^{(1)}(k)=\frac{T}{N}\sum_q G_{\alpha\beta}(k-q)V_{\alpha\beta}^{(1)}(q), \quad (3)$$

where the fluctuation-exchange interaction $V^{(1)}(q)$ is

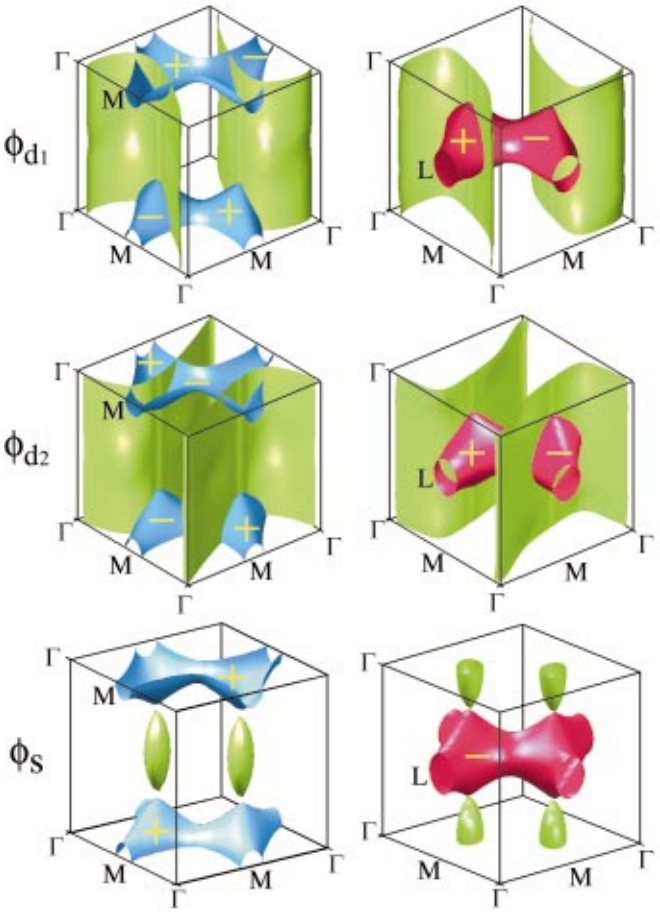

FIG. 3. (Color) The sign of the gap functions ϕ_{d_1}(top), ϕ_{d_2}(middle), and ϕ_s(bottom) for $U=1.5$, $n=1.03$, $t_z=0.65$, $T=0.01$. We have displayed the sign of the gap on the Fermi surface (left panels: bonding band, right panels: antibonding band) along with the nodal planes displayed in green.

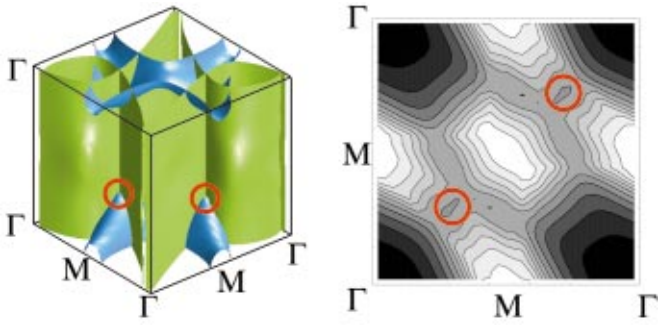

FIG. 4. (Color) Left panel superposes ϕ_{d_1} and ϕ_{d_2} for the bonding band. The right panel plots $|\phi_{d_1}+i\phi_{d_2}|$ for $k_z=0$. The red circles denote point nodes in $\phi_{d_1}+i\phi_{d_2}$.

$$V^{(1)}_{\alpha\beta}(q)=\frac{3}{2}U^2\left[\frac{\chi^{\rm irr}(q)}{1-U\chi^{\rm irr}(q)}\right]_{\alpha\beta}+\frac{1}{2}U^2\left[\frac{\chi^{\rm irr}(q)}{1+U\chi^{\rm irr}(q)}\right]_{\alpha\beta}-U^2\chi^{\rm irr}_{\alpha\beta}(q) \tag{4}$$

with

$$\chi^{\rm irr}_{\alpha\beta}(q)=-\frac{T}{N}\sum_k G_{\alpha\beta}(k+q)G_{\beta\alpha}(k). \tag{5}$$

Here we denote $q\equiv(\mathbf{q},i\epsilon_l)$ with $\epsilon_l=2\pi lT$ being the Matsubara frequency for bosons, and N the number of $\mathbf{k}$ points on a mesh.

With Dyson's equation

$$[G(k)^{-1}]_{\alpha\beta}=[G^0(k)^{-1}]_{\alpha\beta}+\Sigma_{\alpha\beta}(k), \tag{6}$$

where G^0 is the bare Green's function $G^0_{\alpha\beta}(k)=[(i\omega_n+\mu-\epsilon^0_{\mathbf{k}})^{-1}]_{\alpha\beta}$ with $\epsilon^0_{\mathbf{k}}$ the bare energy, we have solved Eqs. (3)–(6) self-consistently.

T_c may be obtained from Eliashberg's equation (for the spin-singlet pairing)

$$\lambda\phi_{\alpha\beta}(k)=-\frac{T}{N}\sum_{k'}\sum_{\alpha',\beta'}V^{(2)}_{\alpha\beta}(k-k')G_{\alpha\alpha'}(k')\times G_{\beta\beta'}(-k')\phi_{\alpha'\beta'}(k'), \tag{7}$$

where ϕ is the gap function and the pairing interaction $V^{(2)}(k)$ is given as

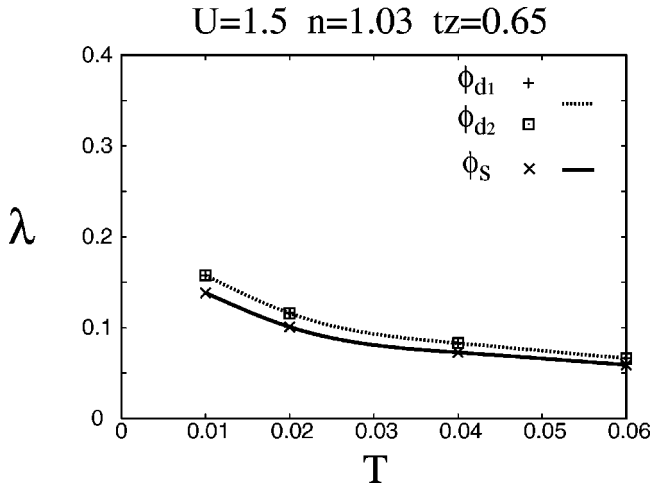

FIG. 5. The eigenvalue of Eliashberg's equation λ versus temperature. The largest solutions are doubly degenerate. Lines in this and following figures are guides to the eye.

$$V^{(2)}_{\alpha\beta}(q)=\frac{3}{2}U^2\left[\frac{\chi^{\rm irr}(q)}{1-U\chi^{\rm irr}(q)}\right]_{\alpha\beta}-\frac{1}{2}U^2\left[\frac{\chi^{\rm irr}(q)}{1+U\chi^{\rm irr}(q)}\right]_{\alpha\beta}+U\delta_{\alpha\beta}. \tag{8}$$

T_c is determined as the temperature at which maximum eigenvalue λ becomes unity.

The susceptibility

$$\chi_{\alpha\beta}(\mathbf{k},0)=\left[\frac{\chi^{\rm irr}(\mathbf{k},0)}{1-U\chi^{\rm irr}(\mathbf{k},0)}\right]_{\alpha\beta}, \tag{9}$$

may be expressed as diagonalized components

$$\chi_{\pm}=\frac{\chi_{AA}+\chi_{BB}}{2}\pm\sqrt{\left[\frac{\chi_{AA}-\chi_{BB}}{2}\right]^2+|\chi_{AB}|^2}. \tag{10}$$

Throughout this study, we take $N=32^3$ $\mathbf{k}$-point meshes, and the Matsubara frequencies ω_n from $-(2N_c-1)\pi T$ to $(2N_c-1)\pi T$ with $N_c=4096$, which gave converged results.

III. RESULT

A. MgB_2

Let us first discuss the spin structure. We have fitted the shape of the Fermi surface to that obtained by the band

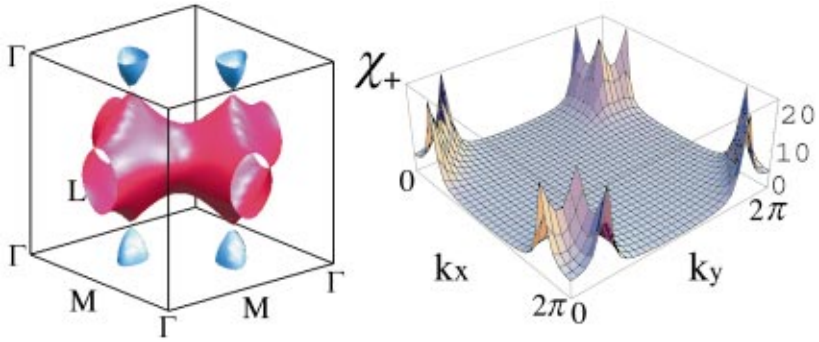

FIG. 6. (Color) Fermi surface (left) and $\chi_+(k_z=\pi)$ (right) for the optimized parameter set of $U=8$, $n=1.15$, $t_z=0.7$ at $T=0.01$, where the pairing symmetry is d wave.

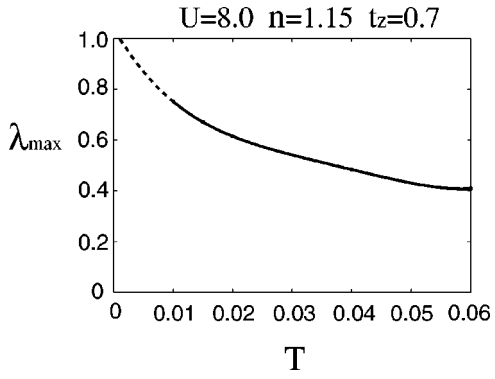

FIG. 7. λ versus temperature for the optimized parameter set employed in the previous figure. The dotted line is a spline extrapolation to lower temperatures.

calculation[19] to have $t_z=0.65$, $n=1.03$, $U=1.5$ at $T=0.01$, where n is band filling ($n=1$ for half filling).[28] The Fermi surface, Fig. 2, consists of two sets of tubular networks corresponding to the bonding and antibonding π bands. The spinsusceptibility $\chi_+(\mathbf{k},0)$ displayed in the same figure shows a sharp peak around $(0,0,\pi)$ reflecting a good nesting along the z direction (arrows in Fig. 2).

Figure 3 shows the gap function obtained from Eliashberg's equation. The solutions having the largest λ are gapless ϕ_{d_1} and ϕ_{d_2}, which are degenerate. As expected from the work of Kuroki and Arita,[18] a *gapful* ϕ_s does exist, although its λ is slightly smaller than that for the d wave. We have called the former solutions "d wave" in that the gap function changes sign as $+-+-$ azimuthally (i.e., within each band), while the latter gap "s wave" in that it does not.

As a hallmark that the scattering of the (intraband) pairs across the interband nesting is exploited, all these solutions indeed have

$$\phi_{AA}(k)\phi_{BB}(k')<0. \tag{11}$$

We can confirm in Eliashberg's Eq. (7) that the sign change across the two bands works favorably in increasing λ if we note $V^{(2)}_{\alpha\beta}(k-k')>0$ [peaked around $\mathbf{k}-\mathbf{k}'=(0,0,\pi)$] and a relation for multiband Green's function $G_{\alpha\beta}(-k)=G^*_{\alpha\beta}(k)$ which gives $G_{AB}(k')G^*_{AB}(-k')>0$.

The fact that the dominant "d-wave" solutions are doubly degenerate can be understood by a group theoretical argument,[29] in which these solutions belong to Γ_6^+ representation for the honeycomb system (while "s wave" belongs to Γ_1^+). The true gap function below T_c to maximize the gap should be a linear combination of the two d waves

$$\phi_{d_1}+i\phi_{d_2}, \tag{12}$$

which breaks the time-reversal symmetry. This combination has *point nodes* on the Fermi surface, which is curious but natural as evident from Fig. 4 which superposes two sets of nodal planes to show how the nodal planes intersect each other along some lines for the doubly degenerate function and how these lines in turn intersect the closed Fermi surface.

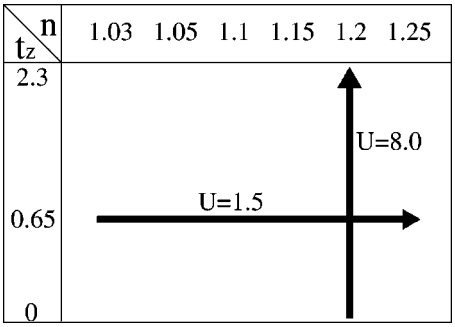

FIG. 8. The paths we have focused on in the present study in the parameter space of the interlayer hopping t_z and the band filling n.

The reason why the "s wave" is only subdominant may be traced back to the Fermi surface, which is rather extended in $\mathbf{k}$ space in this particular case, so that there is an appreciable contribution from the intraband pair scattering that the d wave can exploit.

If we turn to the temperature dependence of λ in Fig. 5, we can see that λ is significantly smaller than unity even for $T\rightarrow 0.01|t|$. This implies that the spin fluctuation alone is not strong enough to realize the d-wave superconductivity in this temperature range for the band filling and t_z taken here.

On the other hand, the λ for the gapful "s-wave" pairing is seen to have nearly the same magnitude as that of the gapless d wave, although λ is again small. Thanks to the absence of nodes on the Fermi surface, this one has a gapful pairing, which is eligible for assisting the phonon-mediated pairing if the electron-phonon interaction is considered on top of the electron-electron interaction.[30] So we conclude that interband spin fluctuations can work cooperatively with intraband phonons to realize a gapful superconductivity.

B. Optimization for the 3D honeycomb lattice

Let us depart from MgB_2 to move on to the strong coupling regime in search of superconductivity from electron repulsion alone. In general, pairing instability mediated by spin fluctuations in 3D systems is definitely weaker than that in 2D systems.[17,31] This has been shown in a FLEX study for the Hubbard model by three of the present authors,[17] who have identified its reason in the $\mathbf{k}$ space volume fraction of the effectively attractive pair scattering region that is much smaller in 3D than in 2D. Furthermore, 3D systems have a strong tendency toward various magnetic orders, so that to identify the 3D systems that favor superconductivity from electron repulsion becomes a challenging problem.

Here we have optimized the pairing instability in the layered honeycomb lattice by varying the interlayer hopping t_z and the band filling n. Namely, we have searched for sets of parameter values that give large values of λ *without* encountering antiferromagnetic instability at low temperatures. The resulting best parameter set is found to be $U=8$, $n=1.15$, $t_z=0.7$ (inset of Fig. 6), for which the Fermi surface and the (inverse) spin susceptibility are shown in Fig. 6. In Fig. 7 we can see that the estimated $T_c\sim 0.001$ ($\lambda_{\max}\rightarrow 1$). The pairing symmetry is again $\phi_{d_1}+i\phi_{d_2}$.

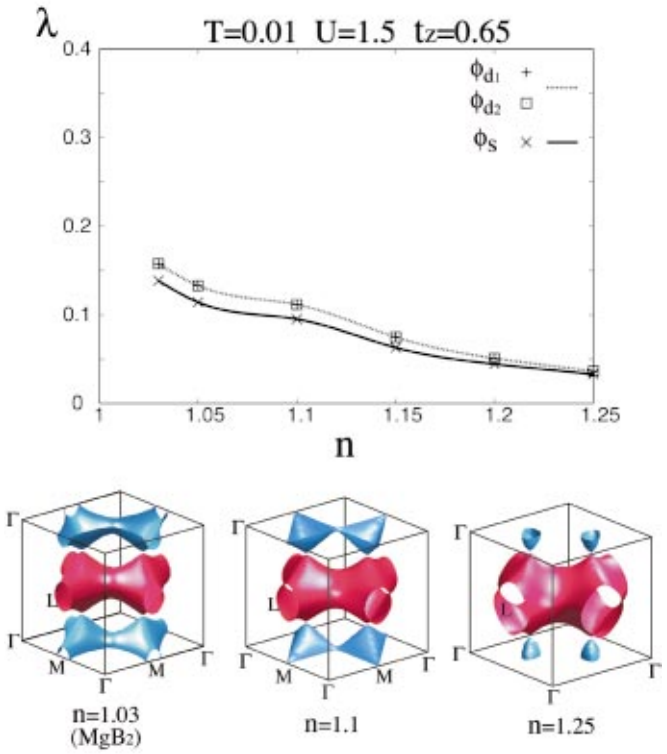

FIG. 9. (Color) λ versus n for $U=1.5$, $t_z=0.65$, $T=0.01$. The d-wave solutions having the largest λ are doubly degenerate.

C. Effect of the interband nesting

Apart from the above optimization, we have systematically explored how the interband nesting affects the pairing in the 3D honeycomb lattice. Since we wish to separate out the effect of the band filling and the hopping in the z direction, we have done this along two paths displayed in Fig. 8. The first path starts from the parameter values corresponding to the $p\pi$ bands in MgB_2, while the second path includes the parameter regime ($t_z<0.2$) which corresponds to GIC except for the value of U. The result along the first path is shown in Fig. 9, where the n dependence of $\lambda_{\max}$ is plotted for $U=1.5$, $t_z=0.65$ at $T=0.01$. We can see that the pairing instability becomes weaker as n is increased, which is natural since the interband nesting becomes degraded along this path.

The result along the second path is displayed in Fig. 10, where λ is plotted as a function of t_z for $n=1.2$ at $T=0.01$. Here we have adopted a rather large $U=8$, because we want to have sizeable λ over a wide range of t_z including the case of bad nesting. There, we have covered both the layered case ($t_z<1$) and a quasi-1D case ($t_z>1$). As indicated in Fig. 10, antiferromagnetism occurs (i.e., $\chi\rightarrow\infty$) when the interband nesting becomes too strong as $t_z\rightarrow 1$ both from below and from above. Before the transition to antiferromagnetism occurs λ increases both from below and from above, indicating that interband 3D nesting is effective, the layered case ($t_z=0.8$) is more advantageous than the case of 2D ($t_z=0$) and quasi-1D ($t_z>1$) on the present path.

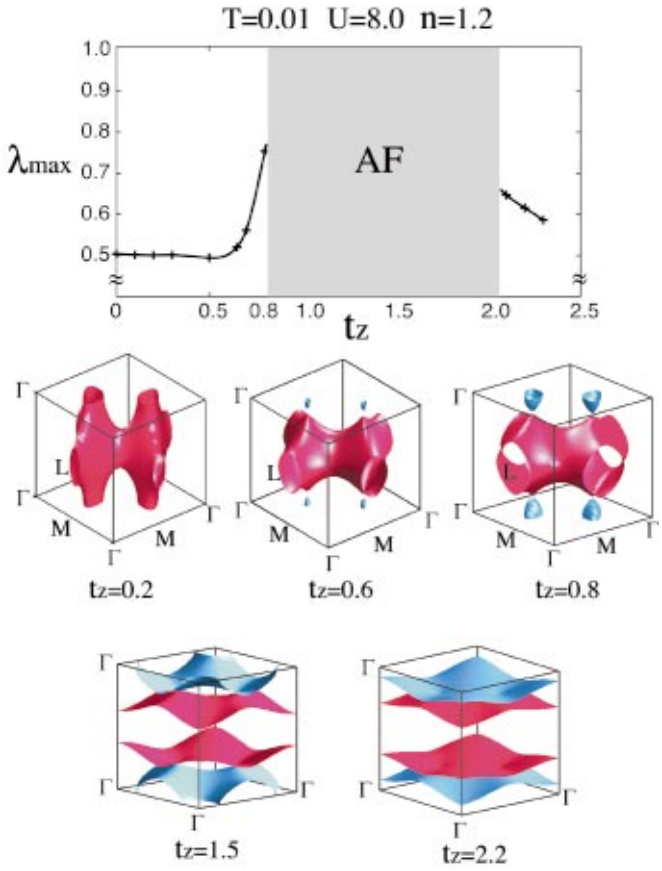

FIG. 10. (Color) λ versus t_z for $U=8$, $n=1.2$, $T=0.01$. The gray region indicates the antiferromagnetic phase. The insets depict the shape of Fermi surface at five points on the horizontal axis.

IV. CONCLUSION

In conclusion, we have studied the possibility of spin-fluctuation mediated superconductivity in 3D honeycomb lattice systematically. We have shown that if we take the parameter set corresponding to the $p\pi$ bands in MgB_2, the spin fluctuation favors the gapful pairing, which suggests that the electron correlation can help the phonon in forming the Cooper pairing. Experimentally, the electron repulsion acting constructively may be confirmed if some phase-sensitive method can detect the gap function having opposite signs in two π bands. When strong enough, the electron repulsion alone will give rise to a d-wave pairing, with a time-reversal broken $\phi_{d_1}+i\phi_{d_2}$ symmetry associated with degenerate representations in the non-Bravais lattice with peculiar point nodes on the Fermi surface.

ACKNOWLEDGMENTS

Numerical calculations were performed at the Computer Center and the ISSP Supercomputer Center of University of Tokyo. This study was in part supported by a Grant-in-aid for scientific research from the Ministry of Education of Japan.

[1] J. Nagamatsu, N. Nakagawa, T. Muranaka, Y. Zenitani, and J. Akimitsu, Nature (London) **410**, 63 (2001).
[2] N. A. W. Holzwarth, S. Rabii, and L.A. Girifalco, Phys. Rev. B **18**, 5190 (1978).
[3] T. Inoshita, K. Nakao, and H. Kamimura, J. Phys. Soc. Jpn. **43**, 1237 (1977).
[4] D. P. DiVincenzo and S. Rabii, Phys. Rev. B **25**, 4110 (1982).
[5] J. H. Schön, C. Kloc, and B. Batlogg, Science **293**, 2432 (2001).
[6] H. J. Choi, D. Roundy, H. Sun, M.L. Cohen, and S.G. Louie, cond-mat/0111182 (unpublished).
[7] D. G. Hinks, H. Claus, and J.D. Jorgensen, Nature (London) **411**, 457 (2001).
[8] S. L. Bud'ko, G. Lapertot, C. Petrovic, C.E. Cunningham, N. Anderson, and P.C. Canfield, Phys. Rev. Lett. **86**, 1877 (2001).
[9] Y. Wang, T. Plackowski, and A. Junod, Physica C **355**, 179 (2001).
[10] F. Bouquet, R.A. Fisher, N.E. Phillips, D.G. Hinks, and J.D. Jorgensen, Phys. Rev. Lett. **87**, 047001 (2001).
[11] T. Takahashi, T. Sato, S. Souma, T. Muranaka, and J. Akimitsu, Phys. Rev. Lett. **86**, 4915 (2001).
[12] S. Tsuda, T. Yokoya, T. Kiss, Y. Takano, K. Togano, H. Kitou, H. Ihara, and S. Shin, Phys. Rev. Lett. **87**, 177006 (2001).
[13] G. Karapetrov, M. Iavarone, W.K. Kwok, G.W. Crabtree, and D.G. Hinks, Phys. Rev. Lett. **86**, 4374 (2001).
[14] P. Szabó, P. Samuely, J. Kačmarčík, T. Klein, J. Marcus, D. Fruchart, S. Miraglia, C. Marcenat, and A. G. M. Jansen, Phys. Rev. Lett. **87**, 137005 (2001).
[15] F. Manzano, A. Carrington, and N. E. Hussey, Phys. Rev. Lett. **88**, 047002 (2002).
[16] X. K. Chen, M. J. Konstantinović, J. C. Irwin, D. D. Lawrie, and J.P. Franck, Phys. Rev. Lett. **87**, 157002 (2001).
[17] R. Arita, K. Kuroki, and H. Aoki, J. Phys. Soc. Jpn. **69**, 1181 (2000); Phys. Rev. B **60**, 14585 (1999).
[18] K. Kuroki and R. Arita, Phys. Rev. B **64**, 024501 (2001).
[19] J. Kortus , I. I. Mazin, K. D. Belashchenko, V. P. Antropov, and L. L. Boyer, Phys. Rev. Lett. **86**, 4656 (2001).
[20] K. Yamaji, J. Phys. Soc. Jpn. **70**, 1476 (2001).
[21] N. Furukawa, J. Phys. Soc. Jpn. **70**, 1483 (2001).
[22] N. E. Bickers, D. J. Scalapino, and S. R. White, Phys. Rev. Lett. **62**, 961 (1989).
[23] N. E. Bickers and D. J. Scalapino, Ann. Phys. (N.Y.) **193**, 206 (1989).
[24] T. Dahm and L. Tewordt, Phys. Rev. B **52**, 1297 (1995).
[25] M. Langer, J. Schmalian, S. Grabowski, and K.H. Bennemann, Phys. Rev. Lett. **75**, 4508 (1995).
[26] S. Koikegami, S. Fujimoto, and K. Yamada, J. Phys. Soc. Jpn. **66**, 1438 (1997).
[27] H. Kontani and K. Ueda, Phys. Rev. Lett. **80**, 5619 (1998).
[28] $U/|t|<2$ is appropriate here because $t\approx 1.7$ eV [K. Voelker, V.I. Anisimov, and T.M. Rice, cond-mat/0103082 (unpublished)] for p_π orbitals in MgB_2, while U for 2p orbitals should be less than ~ 4 eV as estimated for the O2p orbitals in the high-T_C cuprates.
[29] M. Sigrist and K. Ueda, Rev. Mod. Phys. **63**, 239 (1991).
[30] Here we assume that phonons have long wavelength, so that they mainly mediate attractive pairing interaction within each band.
[31] P. Monthoux and G.G. Lonzarich, Phys. Rev. B **59**, 14 598 (1999).